

Adenosine interaction with adenosine receptor A2a promotes gastric cancer metastasis by enhancing PI3K–AKT–mTOR signaling

Linsen Shi^{a,b,†}, Zhaoying Wu^{c,†}, Ji Miao^{d,†}, Shangce Du^b, Shichao Ai^e, En Xu^e, Min Feng^d, Jun Song^{a,f,*}, and Wenxian Guan^{b,d,*}

^aDepartment of Gastrointestinal Surgery, The Affiliated Hospital of Xuzhou Medical University, Xuzhou 221006, People's Republic of China; ^bThe Affiliated Nanjing Drum Tower Clinical College of Nanjing Medical University, Nanjing 210002, People's Republic of China; ^cXuzhou Medical University, Xuzhou 221006, People's Republic of China; ^dDepartment of Gastrointestinal Surgery, The Affiliated Drum Tower Hospital of Nanjing University, Nanjing 210000, People's Republic of China; ^eNanjing University, Nanjing 21000, People's Republic of China; ^fInstitute of Digestive Diseases, Xuzhou Medical University, Xuzhou 221006, People's Republic of China

ABSTRACT The accumulation of adenosine in the tumor microenvironment is associated with tumor progression in many cancers. However, whether adenosine is involved in gastric cancer (GC) metastasis and progression, and the underlying molecular mechanism, is largely unclear. In this study, we find that GC tissues and cell lines had higher A2aR levels than nontumor gastric tissues and cell lines. A2aR expression correlated positively with TNM stage, and associated with poor outcomes. Adenosine enhanced the expression of the stemness and epithelial–mesenchymal transition-associated genes by binding to A2aR. A2aR expression on GC cells promoted metastasis *in vivo*. The PI3K–AKT–mTOR signaling pathway was involved in adenosine-stimulated GC cell migration and invasion. Our results indicate that adenosine promotes GC cell invasion and metastasis by interacting with A2aR to enhance PI3K–AKT–mTOR pathway signaling.

Monitoring Editor

Jonathan Chernoff
Fox Chase Cancer Center

Received: Mar 4, 2019

Revised: Jul 2, 2019

Accepted: Jul 17, 2019

INTRODUCTION

Gastric cancer (GC), an aggressive digestive system disease, is the fifth most frequently diagnosed cancer and the second leading cause of cancer-related death in China (Chen *et al.*, 2016, 2018). Owing to the lack of specific clinical symptoms in the early stage, most patients are diagnosed at an advanced stage (Siegel *et al.*, 2014). Unfortunately, treatment of advanced or metastatic GC has seen little progress to date, and the prognosis remains poor (Cervantes *et al.*, 2013). Metastasis and recurrence represent the

major reason for the poor prognosis of patients with GC (Wang *et al.*, 2016). Therefore, a better understanding of the pathogenesis underlying GC progression and recurrence is essential for developing effective diagnostic and therapeutic strategies for GC.

Epithelial–mesenchymal transition (EMT) is a cell biological program where epithelial cells assume a mesenchymal phenotype and acquire enhanced invasive and metastatic capacity (Pattabiraman *et al.*, 2016; Jin *et al.*, 2017; Wang *et al.*, 2018b). At the same time, the activation of an EMT program enables cells to acquire stem-like properties (Mani *et al.*, 2008; Shuang *et al.*, 2014). Cancer stem cells (CSCs), an aggressive subpopulation of tumor cells with high metastatic potential and profound resistance against conventional anti-cancer therapy, is considered responsible for cancer progression, distant metastasis, and recurrence (Singh and Settleman, 2010; Wang *et al.*, 2017).

Large solid tumors usually develop in a hypoxic tumor microenvironment (TME). In a hypoxic TME, adenosine is catalyzed from ATP in sequential steps mediated by two ectonucleotidases: CD39 and CD73 (Yegutkin, 2008). Once synthesized, adenosine is transferred to the extracellular space and performs its function by binding to four G protein–coupled adenosine receptor subtypes, that is, A1, A2A, A2B, and A3, with different affinities (Hasko *et al.*, 2008). The

This article was published online ahead of print in MBcC in Press (<http://www.molbiolcell.org/cgi/doi/10.1091/mbc.E19-03-0136>) on July 24, 2019.

The authors declare no conflict of interest.

[†]Co-first authors.

*Address correspondence to: Wenxian Guan (guan-wx@163.com); Jun Song (songjunwk@126.com).

Abbreviations used: A2aR, adenosine receptor A2a; CSCs, cancer stem cells; EMT, epithelial–mesenchymal transition; GC, gastric cancer; HIF, hypoxia-inducible factor; MMPs, matrix metalloproteinases; TME, tumor microenvironment.

© 2019 Shi, Wu, Miao, *et al.* This article is distributed by The American Society for Cell Biology under license from the author(s). Two months after publication it is available to the public under an Attribution–Noncommercial–Share Alike 3.0 Unported Creative Commons License (<http://creativecommons.org/licenses/by-nc-sa/3.0>).

"ASCB®," "The American Society for Cell Biology®," and "Molecular Biology of the Cell®" are registered trademarks of The American Society for Cell Biology.

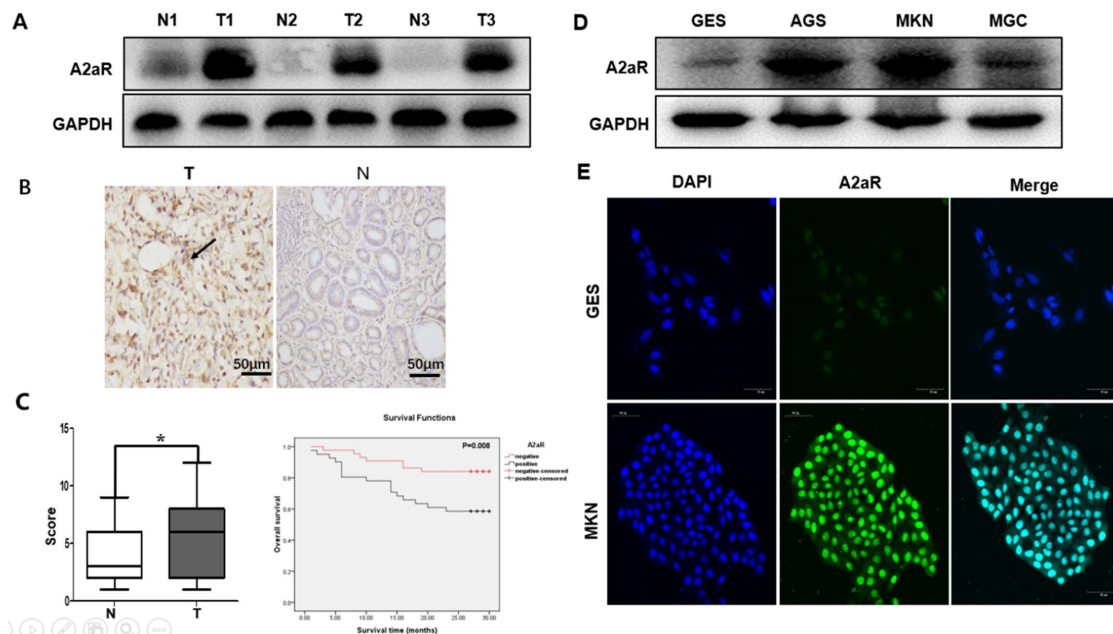


FIGURE 1: High A2aR expression in GC is associated with poor outcomes. Immunoblotting (A) and immunohistochemistry (B) assays of A2aR expression in tissue arrays of tumor (T) and para-tumor (N) normal tissues from 97 patients with GC. Black arrow: A2aR. Scale bar = 50 μ m. *, $P < 0.05$, t test. (C) Kaplan–Meier curves for cumulative survival show a significant association between high A2aR expression in GC and worse prognosis ($P = 0.008$, log-rank test). Immunoblotting (D) and immunofluorescence (E) assays both show higher A2aR expression in GC cell lines than in the nontumorigenic gastric epithelial cell line. Scale bar = 50 μ m.

accumulation of adenosine in the TME is associated with tumor progression, enhanced metastatic potential, and poor prognosis in many cancers (Mittal *et al.*, 2016; Allard *et al.*, 2017; Lupia *et al.*, 2018).

However, whether adenosine is involved in GC metastasis and progression is unclear, as is the underlying molecular mechanism. In the present study, we characterized the expression status of adenosine receptors in GC tissues and cell lines. We found markedly elevated expression of adenosine receptor A2a (A2aR) in both GC tissues and cell lines. Moreover, adenosine promoted GC metastasis and invasion by enhancing cancer cell EMT and stemness. We subsequently investigated the molecular mechanisms involved in these processes, and found that the PI3K (phosphatidylinositol-4,5-bisphosphate 3-kinase catalytic subunit alpha)–AKT–mTOR pathway is involved in adenosine-induced GC metastasis. Finally, using a mouse model of lung metastasis, we comprehensively showed that A2aR expression on cancer cells promotes GC metastasis.

RESULTS

A2aR expression was enhanced in human primary GC tissues and cell lines

To identify whether A2aR is involved in gastric tumorigenesis, we detected its expression in GC tissues and cell lines with immunohistochemical (IHC), Western blotting, and immunofluorescence staining. GC tissues had higher A2aR expression than normal human gastric tissues (Figure 1, A and B). A2aR expression correlated positively with tumor size ($P = 0.032$), N staging ($P < 0.023$), and TNM (According to the 2016 American Association of Cancer [AJCC] TNM staging system) stage ($P = 0.044$), but was not significantly related with other clinicopathological characteristics (Table 1). We analyzed the correlations between A2aR expression and overall survival (OS) time using the Kaplan–Meier method, and found that A2aR-positive status in gastric tissues correlated significantly with OS time ($P = 0.008 < 0.05$;

Figure 1C). Western blotting and immunofluorescence showed that the GC cell lines also had greater A2aR expression than the nontumorigenic gastric epithelial cell line (Figure 1, D and E). These results suggest that aberrant A2aR expression is associated with GC metastasis and may predict poor prognosis.

Adenosine promoted GC cell migration and invasion through the A2aR pathway in vitro

To explore the biological significance of A2aR in GC, MKN45 cells were cocultured with NECA (adenosine derivatives, nonselective adenosine receptor agonists) alone or with 5'-(*N*-ethylcarboxamido) adenosine (NECA) + SCH 58261. Compared with the control or adenosine + ZM241385 (an adenosine A2a antagonist), NECA-treated cells had more pseudopod and cilia growth, indicating stronger migration ability (Figure 2A). The effects of NECA on cell migration and invasion were assessed using Transwell assays. Adenosine significantly increased GC cell migration and invasion (Figure 2B). Furthermore, the wound-healing assay showed obviously enhanced migration in NECA-treated cells (Figure 2C). We also detected the tumor metastasis-related matrix metalloproteinases (MMPs) and found that adenosine increased MMP-2, MMP-7, MMP-9, and MMP-13 expression in the MKN45 cells, but that SCH 58261 blocked this effect (Figure 2D). However, the expression of MMP9, 48 h and 72 h decreased slightly more than 24 h, which may be related to adenosine-induced tumor cell apoptosis (Sargazi *et al.*, 2019; Soleimani *et al.*, 2019). Collectively, these findings demonstrate that adenosine promotes tumor invasion and metastasis in GC through the A2aR pathway.

Adenosine regulated the expression of the stemness and EMT-associated genes through the A2aR pathway in vitro

Given the crucial role of EMT and stemness in cancer invasion and metastasis, we examined the potential effect of adenosine on the

Characteristics	N = 97	A2aR (-)	A2aR (+)	P
Age (yr)				0.641
≤60	41	21	20	
>60	56	26	30	
Gender				0.162
Male	70	37	33	
Female	27	10	17	
Size (cm)				0.032
≤5.0	52	31	21	
>5.0	45	17	28	
Location				0.413
Cardia	31	18	13	
Body	26	12	14	
Antrum	40	17	23	
Differentiation				0.504
Well/well-moderate	18	10	8	
Moderate/poor	79	37	42	
TNM stage				0.044
I/II	26	17	9	
III/IV	71	30	41	
N stage				0.023
N1	38	25	13	
N2	37	14	23	
N3	22	8	14	

P values were calculated by χ^2 test.

TABLE 1: Correlation between clinicopathologic variables and expression of A2aR in GC.

expression of several EMT-related hallmarks and transcription factors. The membrane of NECA-treated MKN45 cells had lower protein levels of the epithelial markers E-cadherin and ZO-1 (zona occludens 1) than the control, but coculture with SCH 58261 repressed this effect. Adenosine markedly increased the expression of the mesenchymal markers, that is, N-cadherin, vimentin, β -catenin, and the EMT transcriptional factors (EMT-TFs), including Snail and Slug, compared with the control or SCH 58261 (Figure 3A). Immunofluorescence assay confirmed these findings (Figure 3B).

Adenosine also resulted in significantly higher expression of the stemness-associated proteins, that is, SOX2 (SRY-box 2), OCT4 (POU class 5 homeobox 1), Nanog, CD44, and CD133, than the control or SCH 58261 (Figure 3, C and D). Colony formation assay confirmed these findings, and SCH 58261 could reverse this effect (Figure 3E). The results suggest that adenosine may induce EMT and enhance the stemness of GC cells to promote metastasis through the A2aR pathway.

GC cell migration and invasion in response to adenosine stimuli depends on PI3K–AKT–mTOR activation

The accumulation of extracellular adenosine is due to the Warburg effect in the hypoxic TME (Vander Heiden *et al.*, 2009). In tumors, hypoxia may cause the switch from cellular respiration to aerobic glycolysis in the mitochondria, eventually leading to PI3K–AKT–

mTOR pathway activation (Caino *et al.*, 2015). We wanted to know whether adenosine regulation of GC cell migration and invasion is related to the PI3K–AKT–mTOR signaling pathway. Accordingly, we detected the expression of the relevant proteins. The p-PI3K, p-AKT, and p-mTOR levels were enhanced in NECA-treated cells, which SCH 58261 could abolish (Figure 4A).

To determine whether the PI3K–AKT–mTOR signaling pathway is involved in adenosine-stimulated GC cell migration and invasion, MKN45 cells were treated with a selective mTOR antagonist (OSI-027) after adenosine treatment. OSI-027 caused near complete suppression of the adenosine-induced GC cell EMT, stemness, and migration (Figure 4, B–D). Together, these data suggest that the PI3K–AKT–mTOR signaling pathway may play an essential role in adenosine-stimulated GC cell migration and invasion.

A2aR promoted metastasis in vivo

We used a human GC tumor xenograft setting to evaluate the role of A2aR expression in controlling metastasis. Sh control (NC) or A2aR KD MKN45 cells were injected into the lateral tail vein of nude mice, and administered A2aRi. Tumor metastasis was examined in vivo by monitoring the fluorescence photon flux. Mice bearing control MKN45 cells had a comparably higher luminescent tumor signal than A2aR-depleted or A2aRi-treated mice (Figure 5A). After the mice had been sacrificed at week 4, we found more and larger micrometastatic lesions in the lungs of the mice that had been injected with Sh control cells, but that A2aR knockdown or A2aRi reduced the lung metastases significantly (Figure 5, B–D). Collectively, our data strongly suggest that inhibiting A2aR either with small-molecule inhibitors or gene knockdown may inhibit metastases in human GC cell lines.

DISCUSSION

In the present study, we found significantly higher A2aR expression in GC tissues and cell lines than in normal human gastric tissues, and A2aR expression was associated with GC metastasis and may predict poor prognosis. Both in vitro and in vivo studies demonstrated that adenosine may induce EMT and enhance GC cell stemness to promote metastasis by binding to A2aR, and that small-molecule inhibitors or gene knockdown of A2aR could abolish this effect near completely. We also demonstrate for the first time that the PI3K–AKT–mTOR signaling pathway is involved in adenosine-stimulated GC cell migration and invasion. Therefore, A2aR may be deemed a key point in GC progress.

Metastasis and recurrence are the most challenging issues in managing patients with GC, but no effective therapies specifically target disease progression to date (Marquardt *et al.*, 2018). Cumulative evidence has shown that tumor metastasis is closely correlated with the TME, in which hypoxia and inflammatory cell infiltration are two main factors (Ackerman and Simon, 2014; Wang *et al.*, 2018a). The stabilization and activation of hypoxia-inducible factor (HIF) responses to hypoxic TME may facilitate tumor growth, angiogenesis, and metastasis (Semenza, 2010). HIF-1 α , a HIF-1 subunit, promotes tumor metastasis by up-regulating the EMT-TFs (Tsai *et al.*, 2014). HIF-1 α overexpression also participates in GC metastasis and is associated with poor prognosis (He *et al.*, 2017; Gan *et al.*, 2018; Zhang *et al.*, 2018). However, accumulating evidence suggests that hypoxia usually leads to massive tumor necrosis but is not sufficient to induce EMT (Kutluk Cenik *et al.*, 2013; Peng *et al.*, 2018), so the underlying mechanism of hypoxia involvement in EMT and GC metastasis remains unclear.

In the hypoxic TME, HIF-1 α activation due to the Warburg effect can increase CD39 and CD73 expression in numerous cells, including regulatory T-cells (Treg), leukocytes, and endothelial cells,

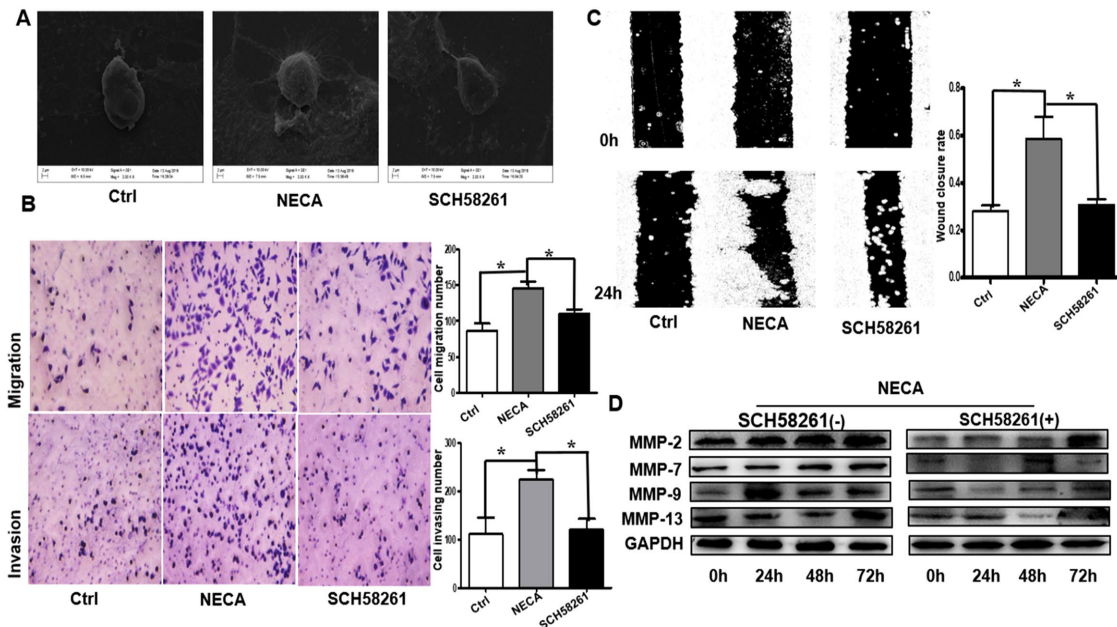


FIGURE 2: Adenosine promotes GC cell invasion and metastasis through the A2aR pathway in vitro. (A) Representative scanning electron microscopy images showing significantly more pseudopodia and cilia growth. (B) Migration (top) and invasion (bottom) Transwell assays showing increased invasive capability of NECA-treated cells compared with control (Ctrl) or NECA + SCH 58261-treated cells. Scale bar = 100 μ m. Bars represent mean \pm SEM of at least three independent quadruplicate experiments. (C) Wound-healing assay in MKN45 cells: the scratch was measured 24 h after the treatments. Bars represent mean \pm SEM of at least three independent quadruplicate experiments. (D) Immunoblot detection of tumor metastasis-related MMPs. Data are the mean \pm SE of triplicate measurements. *, $P < 0.05$, ANOVA.

eventually leading to the accumulation of extracellular adenosine in tumors (Vander Heiden *et al.*, 2009; Sun *et al.*, 2010; Li and Simon, 2013). As adenosine is associated with the progression of many cancers, we wanted to know whether and how it can promote GC

metastasis and progression. The higher A2aR expression in the GC tissues and cell lines in the present study indicate that adenosine may be involved in the progression of many cancers. Subsequently, both in vitro and in vivo studies confirmed that adenosine

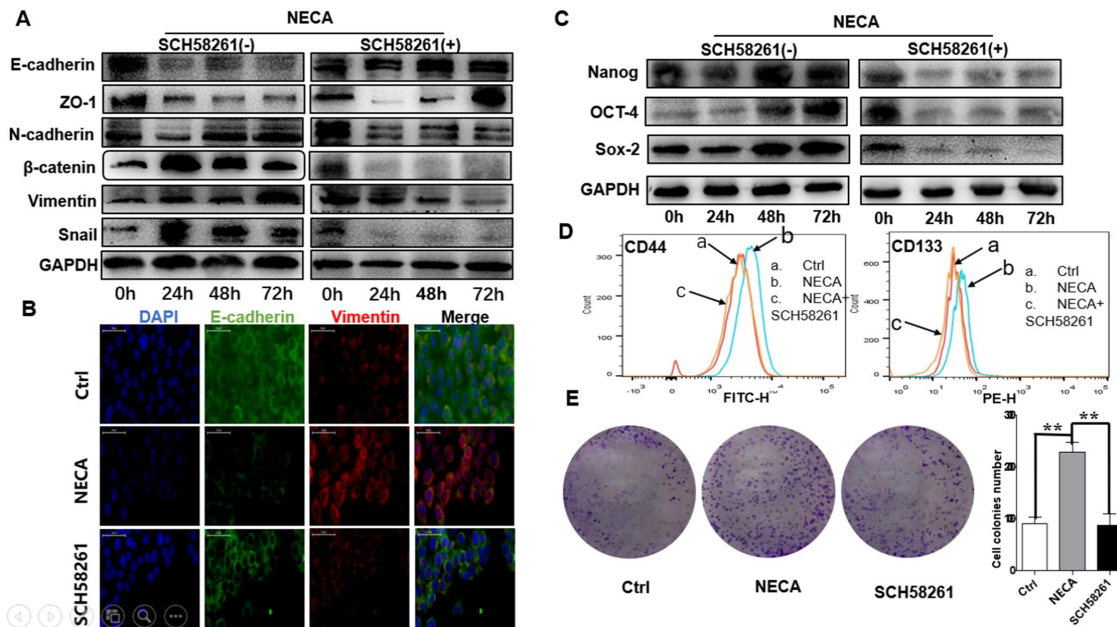


FIGURE 3: Adenosine (NECA) regulates the expression of the stemness and EMT-associated genes through the A2aR pathway in vitro. Epithelial and mesenchymal marker expression was analyzed by immunoblotting (A) and immunofluorescence staining (B). Scale bar = 50 μ m. (C) Immunoblotting detection of the stemness markers. The adenosine-induced increased stemness was confirmed by flow cytometry (D) and colony formation assay (E), but the specific antagonist of A2aR (SCH 58261) could reverse this effect. **, $P < 0.01$, ANOVA. All results are from three independent experiments.

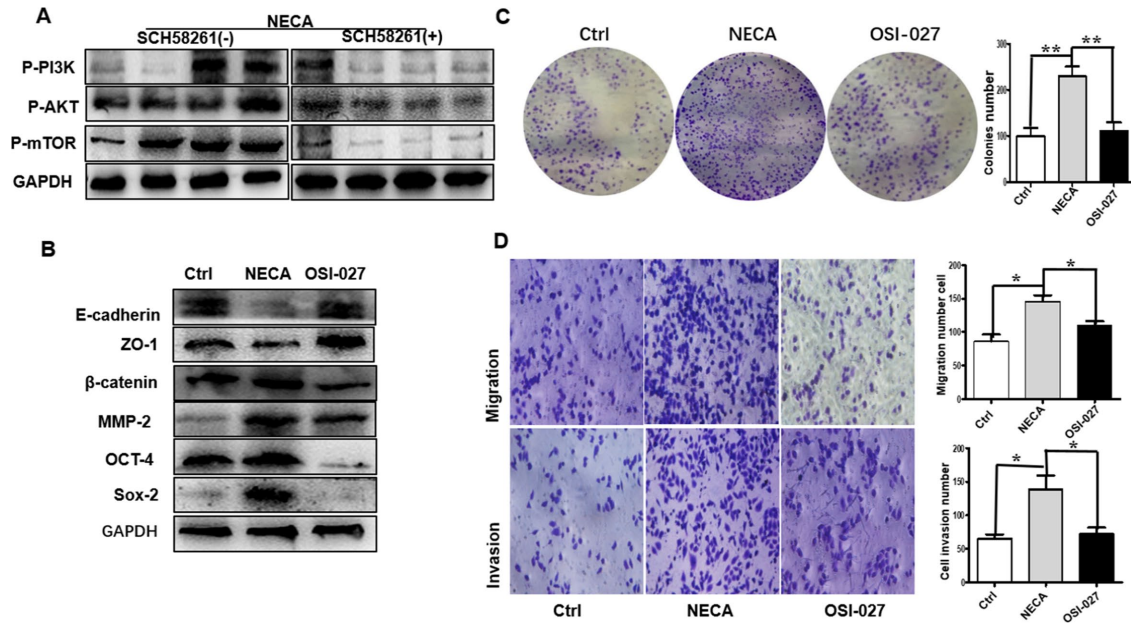


FIGURE 4: Adenosine promotes GC cell metastasis based on PI3K–AKT–mTOR pathway activation. (A) NECA-treated MKN45 cells had higher PI3K, AKT, and mTOR expression than vehicle- or NECA + SCH 58261–treated cells. (B) Immunoblotting detection of MMPs, and epithelial, mesenchymal, and stemness markers after treatment with OSI-027 (2 μM). Colony formation (C) and Transwell (D) assays confirmed the decreased invasive capability and stemness of GC cells after OSI-027 treatment. Data are the mean ± SEM, *, $P < 0.05$, **, $P < 0.01$, ANOVA. All results are from three independent experiments.

can promote GC metastasis and that blocking or knocking down A2aR may abolish this process.

Tumor progression toward invasion and metastasis is a stepwise and multistage process in which EMT may be a major event (Thiery,

2002; Luan *et al.*, 2018). The EMT program is also known as a defined route for the generation of both normal and neoplastic epithelial stem cells (Mani *et al.*, 2008; Guo *et al.*, 2012). CSCs, a subpopulation of cells with the ability to sustain self-renewal, are

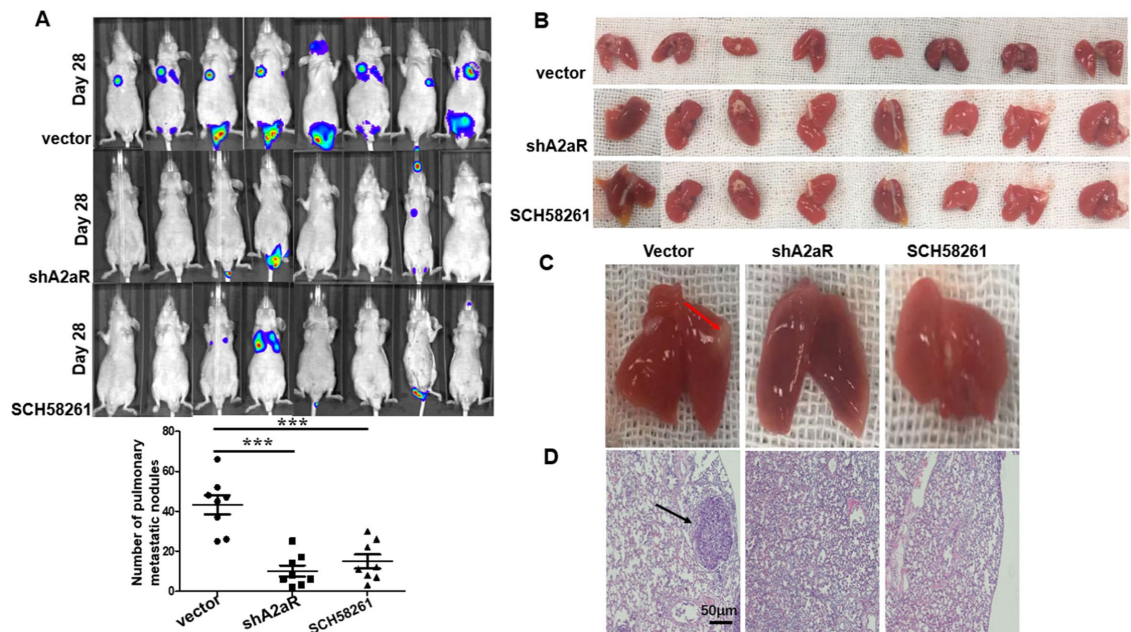


FIGURE 5: Blocking of A2aR on GC cells suppresses lung metastasis in vivo. Short hairpin (Sh) control (negative control [NC]) or A2aR KD MKN45 cells (5×10^5 cells) were injected intravenously in a 200-μl volume into male athymic BALB/c nude mice. In the group of Ctrl or A2aRi, the mice were treated intraperitoneally with vehicle or A2aR inhibitor (SCH58261, 10 mg/kg) two times every week. (A) The photon fluxes were monitored at week 4 after tumor cell injection. (B, C) The lungs in each treatment group were collected and the metastatic burden was quantified by counting colonies on the lung surface 4 wk after tumor cell injection. Results are the mean ± SEM; $n =$ eight mice per group. (D) Representative hematoxylin–eosin staining images of lung tissue sections from each group. Scale bar = 100 μm. ***, $P < 0.001$, ANOVA.

responsible for tumor initiation, invasion, metastasis, recurrence, and resistance to conventional therapeutic modalities (Zhou *et al.*, 2009; Yao *et al.*, 2014). CD44 and CD133 have been recognized as the most common CSC markers in gastric and other cancers (Neuzil *et al.*, 2007; Wei *et al.*, 2016). However, the underlying mechanisms of these processes in GC remain unclear to date. In the present study, we discovered that adenosine can regulate the EMT-associated genes and enhance CD44 and CD133 expression on MKN45 cells and that this effect may occur mainly through the A2aR pathway.

The PI3K–AKT–mTOR signaling pathway is one of the key regulators that support cancer cell survival, expansion, and dissemination (Thorpe *et al.*, 2015; Jia *et al.*, 2018). ADO receptors, belonging to the class A (rhodopsin-like) G protein–coupled receptor (GPCR) superfamily, are classified into A1, A2A, A2B, and A3 groups based on their pharmacologic and functional characteristics (Fredholm *et al.*, 2000). Manipulation of GPCRs with selective ligands may play a fundamental role in regulating various physiological and pathophysiological processes through stimulating downstream signaling, such as PI3K–AKT–mTOR pathway (Franco *et al.*, 2017; De Ceunynck *et al.*, 2018). Here, we found that adenosine significantly enhanced p-PI3K, p-AKT, and p-mTOR levels, but that the A2aR antagonist blocked the activation of this signaling pathway in an obvious manner. The subsequent application of an mTOR antagonist showed that abolishing this signaling pathway can reverse the adenosine-enhanced EMT and stemness in MKN45 cells. Therefore, we may conclude that the accumulation of adenosine in a hypoxic TME can activate the PI3K–AKT–mTOR signaling pathway by binding to A2aR, and then promote EMT and enhance cancer cell stemness, eventually leading to GC metastasis and progression. Other researchers have also found that suppression of the mTOR pathway may significantly attenuate GC proliferation and EMT-induced metastasis (Du *et al.*, 2017; Zhang *et al.*, 2017). However, the contradictory results demonstrated by Matsumoto *et al.* show that HIF-1 α induction under hypoxic conditions inhibits mTOR signaling and up-regulates CD133 expression (Matsumoto *et al.*, 2009). This discrepancy might be explained by the different cellular context of glioma from other cancers.

Overall, our results demonstrate an important role for adenosine in GC progression and metastasis, and may therefore pave the way to a novel approach to treatment strategies for patients with advanced GC. At the same time, A2aR expression correlated positively with stage and OS time, so it may also be a diagnostic and prognostic indicator in patients with GC. However, given the relatively small sample size and short follow-up time in the present study, more research is needed to confirm our conclusion. The regulation of GC progression and metastasis should involve a complex network system; here, we have merely determined that adenosine interaction with A2aR can promote GC metastasis by enhancing PI3K–AKT–mTOR signaling. Accordingly, combining the adenosine–A2aR interaction with other signaling pathways and targets in future studies would also be of interest.

MATERIALS AND METHODS

Human specimens

Primary tumor and adjacent nontumor tissue samples were collected from 97 patients with GC who underwent curative gastrectomy between March 2015 and February 2016 at The Affiliated Hospital of Xuzhou Medical University and were stored at -80°C until tested. Table 1 summarizes the patients' demographic information. Patients who were included in the study had postoperative follow-up for 28–30 mo, and the details and dates of any postoperative recurrence

of GC, morbidity, or mortality were recorded. Oral and written informed consent was obtained from all patients. All clinical studies were approved by the Clinical Research Ethics Committee of Xuzhou Medical University, Jiangsu, China.

Reagents and chemicals

NECA and the A2aR antagonist SCH 58261 were obtained from Sigma (St. Louis, MO). The mTOR antagonist OSI-027 was purchased from MedChem Express (Monmouth Junction, NJ). Purified anti-rabbit A2bR polyclonal antibody was purchased from Bioss Antibodies (Edinburgh, UK). Purified anti-rabbit MMP-2, MMP-7, MMP-9, MMP-13, phosphorylated (p)-mTOR, p-PI3K, p-AKT, A2aR, and FITC-IgG (fluorescein isothiocyanate–immunoglobulin G) fluorescent secondary antibody were purchased from Abcam (Cambridge, UK). The EMT Antibody Sampler Kit was purchased from Cell Signaling Technology (Danvers, MA).

In vitro treatment of cell lines

The GES-1 human gastric normal epithelial mucosa cell line and the GC cell lines MKN45, MGC803, and AGS were purchased from the Chinese Academy of Sciences (Beijing, China) in 2015. All cell lines were cultured in RPMI 1640 medium (Life Technologies, Gaithersburg, MD) supplemented with 10% fetal bovine serum (FBS; Life Technologies), 1% GlutaMAX (Life Technologies), and 1% penicillin/streptomycin (Life Technologies) and incubated in 5% CO₂ at 37°C. The cell lines were treated 24 h postseeding with vehicle (dimethyl sulfoxide), 1 μM NECA, or 1 μM NECA + 1 μM SCH 58261 as previously described (Young *et al.*, 2018).

IHC detection of A2aR in human gastric tissue

IHC detection of A2aR was performed using a streptavidin–peroxidase conjugate method according to the manufacturer's (Beijing Sequoia Jinqiao) instructions. Briefly, after deparaffinization, rehydration in graded ethanol, antigen retrieval, and blocking, slides were incubated with anti-A2aR mAb (1:150) at 4°C overnight. After washing with phosphate-buffered saline (PBS), samples were labeled with horseradish peroxidase (HRP) secondary antibody (SP-9001; Beijing Sequoia Jinqiao, Beijing, China) at room temperature for 1 h. The sections were then stained with diaminobenzidine tetrahydrochloride substrate (Beijing Sequoia Jinqiao) and counterstained with hematoxylin, and consequently dehydrated in graded ethanol. An integral method was applied to evaluate the expression of A2aR: <25% positive cells scored as 1; 25%–50% as 2; 50%–75% as 3; and >75% as 4. Cell color was assessed according to the following criteria: 0 (no staining), 1 (weak staining), 2 (moderate staining), and 3 (strong staining). The two integrals were multiplied and positive expression was defined as a score of >5; negative expression was defined as a score of ≤ 5 . Two independent pathologists blinded to the patient characteristics scored the staining assessments independently.

Immunoblotting assays

MKN45 cells were treated as described above; after 48 h, the cells were lysed in radioimmunoprecipitation assay buffer (Sigma). Total protein concentrations were detected using a bicinchoninic acid protein assay kit (Beyotime, Shanghai, China). Total protein was separated by 10% SDS–PAGE and transferred to polyvinylidene fluoride membranes (Millipore, Billerica, MA). Then, the membranes were blocked with 8% nonfat milk for 2 h at room temperature. The specific primary antibodies were cultured with the membranes at 4°C overnight. The membranes were incubated with goat anti-rabbit IgG–HRP (1:4000; Proteintech) for 2 h. Finally, the blots were

visualized using a Chemiluminescent Substrate kit (Thermo Scientific) and the ChemiDoc MP Imaging System (Bio-Rad).

Immunofluorescence staining

After 48-h treatment, MKN45 cells grown on coverslips were fixed with ice-cold 4% methanol for 15 min, permeabilized for 15 min with 0.3% Triton, blocked for 30 min with 10% bovine serum albumin, and incubated overnight at 4°C with primary antibodies against A2aR, E-cadherin, vimentin, and N-cadherin (all, 1:100). Then, the cells were incubated at 37°C for 1 h with FITC–IgG fluorescent secondary antibody (1:200).

Scanning electron microscopy

After 48-h treatment, the cells in each group were cleaned by immersion in PBS three times and fixed in 3% glutaraldehyde overnight. Then, the cells were dehydrated with 30%–100% gradient ethanol at 15 min per dehydration step. Next, the samples were observed using a scanning electron microscope (EVO MA10/LS10 ZX-01; Zeiss, Oberkochen, Germany).

Transwell and invasion assays

The Transwell assays and invasion assays were conducted using Millicell Hanging Biocoat Matrigel and Control chambers (24-well insert, 8- μ m pore size) according to the manufacturer's instructions (BD Biosciences). Briefly, 5×10^4 cells in 200 μ l serum-free DMEM were loaded in the upper chambers of the Transwell chamber. Then, 600 μ l DMEM supplemented with 10% FBS was loaded in the lower chamber. At 24 h after treatment, the cells on the underside of the membrane were stained with 0.1% crystal violet and counted under a microscope in five random high-power fields.

Wound-healing migration assays

Briefly, 5×10^5 cells per well in RPMI 1640 medium were seeded in a six-well chamber slide. Scratches were made down the middle of the slides using a sterile 10- μ l pipette tip. After scratching, the well was gently washed with medium to remove the detached cells. After treatment, images were obtained at 0 and 24 h using a microscope. Wound closure was evaluated and calculated as follows: wound closure = [area of gap (0 h) – area of gap (24 h)]/area of gap (0 h).

Colony formation assay

Single-cell suspensions of MKN45 cells (200 cells/well) were seeded in a six-well chamber slide. Vehicle, NECA, or NECA + SCH 58261 were added to the suspension cultures on days 1, 4, and 7 after seeding in each group. Colony formation was assessed 14 d after seeding.

Fluorescence-activated cell sorting of CD44 and CD133 stemness marker expression

After 48-h treatment, MKN45 cells were trypsinized for surface marker analysis by flow cytometry. The cells were resuspended and incubated for 30 min at room temperature with anti-CD44–FITC (eBiosciences, Waltham, MA) and anti-CD133–phycoerythrin (PE; eBiosciences). Flow cytometry was performed using a BD flow cytometer (BD, Franklin Lakes, NJ) equipped with Expo32 software (Beckman Coulter).

Lentiviral knockdown (KD) of A2aR

Human A2aR was knocked down using short hairpin RNA (shRNA) lentiviral particles from GeneChem Life Sciences (Shanghai, China)

as per the manufacturer's instructions. MKN45 cells transfected with control luciferase shRNA lentivirus (GenePharma, Shanghai, China), were cultured in a 24-well plate (5×10^4 cells/ml) and transiently transfected with the shRNA lentivirus the next day at a multiplicity of infection (MOI) of 50. The cells were then sorted in three cycles with 2, 4, and 6 μ g/ml puromycin. A2aR knockdown was determined by turbo-GFP (green fluorescent protein) expression and immunoblotting.

In vivo metastasis assay

Male athymic BALB/c nude mice (5 wk old) were used for the animal studies. For the experimental metastasis, short hairpin (Sh) control (negative control [NC]) or A2aR KD MKN45 cells (5×10^5 cells) were injected intravenously in a 200- μ l volume into the mice. In the group of Ctrl or A2aRi, the mice were treated intraperitoneally with vehicle or A2aR inhibitor (SCH 58261, 10 mg/kg) two times every week as described previously (Young *et al.*, 2017). An IVIS Lumina in vivo imaging system (Xenogen, Alameda, CA) was used to measure the volumes of lung metastasis noninvasively. The lungs were harvested on day 30, and macrometastases on the lung surface were counted using a dissecting microscope.

Statistical analysis

All numerical data are presented as the mean \pm SEM; statistical analyses were carried out using nonparametric analysis of variance (ANOVA) between groups, followed by Dunnett's post hoc test. The relationship between A2aR expression and clinicopathological factors were analyzed using the chi-square test. Univariate analysis of prognostic factors was conducted using the Kaplan–Meier method and log-rank test. All experiments were repeated at least three times independently. Statistical analyses applied GraphPad Prism (La Jolla, CA). A difference was considered significant at $P < 0.05$.

ACKNOWLEDGMENTS

This study was supported by the “Top Six Talents” project of Jiangsu Province (2014-WSW-032) and the Natural Science Foundation of Jiangsu Province (BK201508).

REFERENCES

- Ackerman D, Simon MC (2014). Hypoxia, lipids, and cancer: surviving the harsh tumor microenvironment. *Trends Cell Biol* 24, 472–478.
- Allard D, Turcotte M, Stagg J (2017). Targeting A2 adenosine receptors in cancer. *Immunol Cell Biol* 95, 333–339.
- Caino MC, Ghosh JC, Chae YC, Vaira V, Rivadeneira DB, Favarsani A, Rampini P, Kossenkov AV, Aird KM, Zhang R, *et al.* (2015). PI3K therapy reprograms mitochondrial trafficking to fuel tumor cell invasion. *Proc Natl Acad Sci USA* 112, 8638–8643.
- Cervantes A, Roda D, Tarazona N, Roselló S, Pérez-Fidalgo JA (2013). Current questions for the treatment of advanced gastric cancer. *Cancer Treat Rev* 39, 60–67.
- Chen JG, Chen HZ, Zhu J, Yang YL, Zhang YH, Huang PX, Chen YS, Zhu CY, Yang LP, Shen K, *et al.* (2018). Cancer survival in patients from a hospital-based cancer registry, China. *J Cancer* 9, 851–860.
- Chen W, Zheng R, Baade PD, Zhang S, Zeng H, Bray F, Jemal A, Yu XQ, He J (2016). Cancer statistics in China, 2015. *CA Cancer J Clin* 66, 115–132.
- De Ceunynck K, Peters CG, Jain A, Higgins SJ, Aisiku O, Fitch-Tewfik JL, Chaudhry SA, Dockendorff C, Parikh SM, Ingber DE, *et al.* (2018). PAR1 agonists stimulate APC-like endothelial cytoprotection and confer resistance to thromboinflammatory injury. *Proc Natl Acad Sci USA* 30, 115, E982–E991.
- Du C, Li DQ, Li N, Chen L, Li SS, Yang Y, Hou MX, Xie MJ, Zheng ZD (2017). DDX5 promotes gastric cancer cell proliferation in vitro and in vivo through mTOR signaling pathway. *Sci Rep* 7, 42876.
- Franco R, Martínez-Pinilla E, Navarro G, Zamarbide M (2017). Potential of GPRPs to modulate MAPK and mTOR pathways in Alzheimer's disease. *Prog Neurobiol* 149–150, 21–38.

- Fredholm BB, Arslan G, Halldner L, Kull B, Schulte G, Wasserman W (2000). Structure and function of adenosine receptors and their genes, Naunyn-Schmiedeberg's Arch Pharmacol 362, 364–374.
- Gan L, Meng J, Xu M, Liu M, Qi Y, Tan C, Wang Y, Zhang P, Weng W, Sheng W, et al. (2018). Extracellular matrix protein 1 promotes cell metastasis and glucose metabolism by inducing integrin β 4/FAK/SOX2/HIF-1 α signaling pathway in gastric cancer. *Oncogene* 37, 744–755.
- Guo W, Keckesova Z, Donaher JL, Shibue T, Tischler V, Reinhardt F, Itzkovitz S, Noske A, Zürrer-Härdi U, Bell G, et al. (2012). Slug and Sox9 cooperatively determine the mammary stem cell state. *Cell* 148, 1015–1028.
- Hasko G, Linden J, Cronstein B, Pacher P (2008). Adenosine receptors: therapeutic aspects for inflammatory and immune diseases. *Nat Rev Drug Discov* 7, 759–770.
- He C, Wang L, Zhang J, Xu H (2017). Hypoxia-inducible microRNA-224 promotes the cell growth, migration and invasion by directly targeting RASSF8 in gastric cancer. *Mol Cancer* 16, 35.
- Jia L, Huang S, Yin X, Zan Y, Guo Y, Han L (2018). Quercetin suppresses the mobility of breast cancer by suppressing glycolysis through Akt-mTOR pathway mediated autophagy induction. *Life Sci* 208, 123–130.
- Jin K, Li T, van Dam H, Zhou F, Zhang L (2017). Molecular insights into tumour metastasis: tracing the dominant events. *J Pathol* 241, 567–577.
- Kutluk Cenik B, Ostapoff KT, Gerber DE, Brekken RA (2013). BIBF 1120 (nintedanib), a triple angiokinase inhibitor, induces hypoxia but not EMT and block progression of preclinical models of lung and pancreatic cancer. *Mol Cancer Ther* 12, 992–1001.
- Li B, Simon MC (2013). Molecular pathways: targeting MYC-induced metabolic reprogramming and oncogenic stress in cancer. *Clin Cancer Res* 19, 5835–5841.
- Luan M, Chang J, Pan W, Chen Y, Li N, Tang B (2018). Simultaneous fluorescence visualization of EMT and apoptosis processes in tumor cells for evaluating the impact of EMT on drug efficacy. *Anal Chem* 90, 10951–10957.
- Lupia M, Angiolini F, Bertalot G, Freddi S, Sachsenmeier KF, Chisci E, Kutryb-Zajac B, Confalonieri S, Smolenski RT, Giovannoni R, et al. (2018). CD73 regulates stemness and epithelial-mesenchymal transition in ovarian cancer-initiating cells. *Stem Cell Rep* 10, 1412–1425.
- Mani SA, Guo W, Liao MJ, Eaton EN, Ayyanan A, Zhou AY, Brooks M, Reinhardt F, Zhang CC, Shipitsin M, et al. (2008). The epithelial-mesenchymal transition generates cells with properties of stem cells. *Cell* 133, 704–715.
- Marquardt S, Solanki M, Spitschak A, Vera J, Pützer BM (2018). Emerging functional markers for cancer stem cell-based therapies: understanding signaling networks for targeting metastasis. *Semin Cancer Biol* 30, S1044–S1579.
- Matsumoto K, Arai T, Tanaka K, Kaneda H, Kudo K, Fujita Y, Tamura D, Aomatsu K, Tamura T, Yamada Y, et al. (2009). mTOR signal and hypoxia-inducible factor-1 α regulate CD133 expression in cancer cells. *Cancer Res* 69, 7160–7164.
- Mittal D, Sinha D, Barkauskas D, Young A, Kalimutho M, Stannard K, Caramia F, Haibe-Kains B, Stagg J, Khanna KK, et al. (2016). Adenosine 2B receptor expression on cancer cells promotes metastasis. *Cancer Res* 76, 4372–4382.
- Neuzil J, Stantic M, Zabalova R, Chladova J, Wang X, Prochazka L, Dong L, Andera L, Ralph SJ (2007). Tumour-initiating cells vs. cancer “stem” cells and CD133: what's in the name? *Biochem Biophys Res Commun* 355, 855–859.
- Pattabiraman DR, Bierie B, Kober KI, Thiru P, Krall JA, Zill C, Reinhardt F, Tam WL, Weinberg RA (2016). Activation of PKA leads to mesenchymal-to-epithelial transition and loss of tumor-initiating ability. *Science* 351, 6277.
- Peng JM, Bera R, Chiou CY, Yu MC, Chen TC, Chen CW, Wang TR, Chiang WL, Chai SP, Wei Y, et al. (2018). Actin cytoskeleton remodeling drives epithelial-mesenchymal transition for hepatoma invasion and metastasis. *Hepatology* 67, 2226–2243.
- Sargazi S, Saravani R, Zavar Reza J, Zarei Jaliani H, Galavi H, Moudi M, Abtahi NA (2019). Novel poly (adenosine diphosphate-ribose) polymerase (PARP) inhibitor, AZD2461, down-regulates VEGF and induces apoptosis in prostate cancer cells. *Iran Biomed J* 23, 312–323.
- Semenza GL (2010). Defining the role of hypoxia-inducible factor 1 in cancer biology and therapeutics. *Oncogene* 29, 625–634.
- Shuang ZY, Wu WC, Xu J, Lin G, Liu YC, Lao XM (2014). Transforming growth factor- β 1-induced epithelial-mesenchymal transition generates ALDH-positive cells with stem cell properties in cholangiocarcinoma. *Cancer Lett* 354, 320–328.
- Siegel R, Ma J, Zou Z, Jemal A (2014). Cancer statistics, 2014. *CA Cancer J Clin* 64, 9–29.
- Singh A, Settleman J (2010). EMT, cancer stem cells and drug resistance: an emerging axis of evil in the war on cancer. *Oncogene* 29, 4741–4751.
- Soleimani A, Bahreyni A, Roshan MK, Soltani A, Ryzhikov M, Shafiee M, Soukhtanloo M, Jaafari MR, Mashkani B, Hassanian SM, et al. (2019). Therapeutic potency of pharmacological adenosine receptors agonist/antagonist on cancer cell apoptosis in tumor microenvironment, current status, and perspectives. *J Cell Physiol* 234, 2329–2336.
- Sun X, Wu Y, Gao W, Enjyoji K, Csizmadia E, Müller CE, Murakami T, Robson SC (2010). CD39/ENTPD1 expression by CD4⁺ FoxP3⁺ regulatory T cells promotes hepatic metastatic tumor growth in mice. *Gastroenterology* 139, 1030–1040.
- Thiery JP (2002). Epithelial-mesenchymal transitions in tumour progression. *Nat Rev Cancer* 2, 442–454.
- Thorpe LM, Yuzugullu H, Zhao JJ (2015). PI3K in cancer: divergent roles of isoforms, modes of activation, and therapeutic targeting. *Nat Rev Cancer* 15, 7–24.
- Tsai YP, Chen HF, Chen SY, Cheng WC, Wang HW, Shen ZJ, Song C, Teng SC, He C, Wu KJ (2014). TET1 regulates hypoxia-induced epithelial-mesenchymal transition by acting as a co-activator. *Genome Biol* 15, 513.
- Vander Heiden MG, Cantley LC, Thompson CB (2009). Understanding the Warburg effect: the metabolic requirements of cell proliferation. *Science* 324, 1029–1033.
- Wang X, Luo G, Zhang K, Cao J, Huang C, Jiang T, Liu B, Su L, Qiu Z (2018a). Hypoxic tumor-derived exosomal miR-301a mediates M2 macrophage polarization via PTEN/PI3K γ to promote pancreatic cancer metastasis. *Cancer Res* 78, 4586–4598.
- Wang D, Plukker JTM, Coppes RP (2017). Cancer stem cells with increased metastatic potential as a therapeutic target for esophageal cancer. *Semin Cancer Biol* 44, 60–66.
- Wang L, Saci A, Szabo PM, Castillo-Martin M, Domingo-Domenech J, Siefker-Radtke A, Sharma P, Sfakianos JP, Gong Y, et al. (2018b). EMT- and stroma-related gene expression and resistance to PD-1 blockade in urothelial cancer. *Nat Commun* 9, 3503.
- Wang L, Yin J, Wang X, Shao M, Duan F, Wu W, Peng P, Jin J, Tang Y, Ruan Y, et al. (2016). C-type lectin-like receptor 2 suppresses AKT signaling and invasive activities of gastric cancer cells by blocking expression of PI3K subunits. *Gastroenterology* 150, 1183–1195.
- Wei B, Sun X, Geng Z, Shi M, Chen Z, Chen L, Wang Y, Fu X (2016). Isoproterenol regulates CD44 expression in gastric cancer cells through STAT3/MicroRNA373 cascade. *Biomaterials* 105, 89–101.
- Yao HJ, Zhang YG, Sun L, Liu Y (2014). The effect of hyaluronic acid functionalized carbon nanotubes loaded with salinomycin on gastric cancer stem cells. *Biomaterials* 35, 9208–9223.
- Yegutkin GG (2008). Nucleotide- and nucleoside-converting ectoenzymes: important modulators of purinergic signalling cascade. *Biochim Biophys Acta* 1783, 673–694.
- Young A, Ngiow SF, Gao Y, Patch AM, Barkauskas DS, Messaoudene M, Lin G, Coudert JD, Stannard KA, Zitvogel L, et al. (2018). A2AR adenosine signaling suppresses natural killer cell maturation in the tumor microenvironment. *Cancer Res* 78, 1003–1016.
- Young A, Ngiow SF, Madore J, Reinhardt J, Landsberg J, Chitsazan A, Rautela J, Bald T, Barkauskas DS, Ahern E, et al. (2017). Targeting adenosine in BRAF-mutant melanoma reduces tumor growth and metastasis. *Cancer Res* 77, 4684–4696.
- Zhang P, Tang W M, Zhang H, Li YQ, Peng Y, Wang J, Liu GN, Huang XT, Zhao JJ, Li G, et al. (2017). MiR-646 inhibited cell proliferation and EMT-induced metastasis by targeting FOXK1 in gastric cancer. *Br J Cancer* 117, 525.
- Zhang J, Wu Y, Lin YH, Guo S, Ning PF, Zheng ZC, Wang Y, Zhao Y (2018). Prognostic value of hypoxia-inducible factor-1 alpha and prolyl 4-hydroxylase beta polypeptide overexpression in gastric cancer. *World J Gastroenterol* 24, 2381–2391.
- Zhou BB, Zhang H, Damelin M, Geles KG, Grindley JC, Dirks PB (2009). Tumour-initiating cells: challenges and opportunities for anticancer drug discovery. *Nat Rev Drug Discov* 8, 806–823.